Plant Physiology and Biochemistry 144 (2019) 22–34

Contents lists available at ScienceDirect

Plant Physiology and Biochemistry

journal homepage: www.elsevier.com/locate/plaphy

Research article

Effects of soil rewatering on mesophyll and stomatal conductance and the associated mechanisms involving leaf anatomy and some physiological activities in Manchurian ash and Mongolian oak in the Changbai Mountains

Kai Zhu[a,b], Fenghui Yuan[a], Anzhi Wang[a], Hong Yang[a], Dexin Guan[a,*], Changjie Jin[a], Hongxia Zhang[a,b], Yushu Zhang[c], Jiabing Wu[a]

[a] *Key Laboratory of Forest Ecology and Management, Institute of Applied Ecology, Chinese Academy of Sciences, Shenyang, 110016, China*
[b] *University of Chinese Academy of Sciences, Beijing, 100049, China*
[c] *The Institute of Atmospheric Environment, China Meteorological Administration, Shenyang, 110016, China*

ARTICLE INFO

Keywords:
Mesophyll conductance
Stomatal conductance
Water stress
Soil rewatering
Leaf anatomy
Physiological activities

ABSTRACT

The recoveries of mesophyll (g_m) and stomatal conductance to CO_2 (g_{sc}) after soil rewatering have received considerable attention in recent years, but the recovery mechanisms involving leaf anatomy and physiological activities are poorly understood. Moreover, it is also unclear whether leaf gas-phase conductance (g_{ias}) or liquid-phase conductance (g_{liq}) is the main factor promoting g_m recovery. By simultaneously using gas exchange and chlorophyll fluorescence, we measured the recoveries of g_m and g_{sc} in saplings of Manchurian ash (*Fraxinus mandshurica* Rupr.) and Mongolian oak (*Quercus mongolica* Fish. ex Ledeb) exposed to two initial water stress (medium water stress, MW, and severe water stress, SW) and following rewatering. Furthermore, leaf anatomical characteristics and the activities of aquaporin (AQP) and carbonic anhydrase (CA) were measured to explain the mechanisms of g_m and g_{sc} recoveries. The results showed that (i) both g_m and g_{sc} were partly recovered after rewatering, and the recoveries decreased with initial water stress in both species. (ii) The g_m recovery was much greater in Mongolian oak than in Manchurian ash, while the g_{sc} recovery was much greater in Manchurian ash. Consequently, the photosynthesis recovery in Manchurian ash was mostly affected by g_{sc} recovery, while that in Mongolian oak was mostly affected by g_m recovery. (iii) The g_m recovery mainly resulted from the great increase in leaf g_{liq} after rewatering rather than that in g_{ias}, as g_{ias} had a negative effect on g_m recovery. The stomatal opening status improved after rewatering, as the stomatal pore size (SS) increased, greatly promoting g_{sc} recovery. In addition, the activities of both AQP and CA increased after rewatering, which improved CO_2 transmembrane transports and greatly promoted g_m and g_{sc} recoveries.

1. Introduction

Photosynthesis is the basis of various functions in plants, including carbon sequestration and wood production, and it is seriously restricted by water deficit (Quick et al., 1992; Epron et al., 1995; Lawlor and Cornic, 2002; Monclus et al., 2006; Chaves et al., 2009). With rapid changes in precipitation patterns, soil drought events have become more frequent, longer in duration and more intense during the past few decades (Luterbacher et al., 2004; Dore, 2005; Joos and Spahni, 2008; Allen et al., 2013) and have had strong effects on the photosynthesis. Soil drought inhibits photosynthesis physiologically by affecting gas exchange inside the leaf, mainly by decreasing stomatal conductance to CO_2 (g_{sc}) and mesophyll conductance (g_m) in the CO_2 diffusion pathway (Grassi and Magnani, 2005; Flexas et al., 2008, 2009; Galle et al., 2009), since atmospheric CO_2 participates in photosynthesis and must pass through stomata and mesophyll intercellular spaces (Flexas et al., 2008; Galle et al., 2007; Haldimann et al., 2008). Therefore, it is of great significance to explore the relationship between photosynthesis and drought-rewatering events. Furthermore, the relationships between leaf CO_2 diffusion conductance (g_m and g_{sc}) and soil water availability have received much attention.

Similar to the focus on g_{sc} in in-depth studies for several decades, the response of g_m to water stress has received considerable attention in recent years (Flexas et al., 2002, 2006; 2009; Rho et al., 2012), and a few studies have also reported the effects of soil rewatering on both g_m and g_{sc} (Warren, 2006; Galle et al., 2007; Blackman et al., 2009; Brien

* Corresponding author. 72 Wenhua Road, Institute of Applied Ecology, Chinese Academy of Sciences, Shenyang, China.
E-mail address: dxguan@iae.ac.cn (D. Guan).

https://doi.org/10.1016/j.plaphy.2019.09.025
Received 28 June 2019; Received in revised form 17 August 2019; Accepted 17 September 2019
Available online 19 September 2019
0981-9428/ © 2019 Elsevier Masson SAS. All rights reserved.

et al., 2014). For instance, leaf g_m in Richter-110 (*Vitis. berlandieri* × *Vitis. rupestris*) plants decreased by more than 90% during exposure to water stress, but it completely recovered 2 days after rewatering (Flexas et al., 2009). Cano et al. (2014) also found that the complete recovery of A_n after rewatering was characterized by a quicker recovery of g_m and a slower recovery of g_{sc} in two species of *Eucalyptus* plants. However, in *Nicotiana sylvestris* L. plants grown outdoors, a drought-induced decline in g_m did not completely recover after 7 days of rewatering in summer, while g_{sc} was fully recovered (Galle et al., 2009). The g_m and g_{sc} of *Olea. europaea* L. var. Manzanilla plants were not fully recovered even after 46 days of rewatering (Perez-Martin et al., 2011). Therefore, the recovery of g_m and g_{sc} may be species dependent due to differences in physiological functions determined by morphological structures.

The reasons for declines in g_m and g_{sc} during periods of soil drought had been studied extensively, but the g_m and g_{sc} recovery mechanisms had rarely been reported. We believe that the recoveries of g_m and g_{sc} are greatly affected by leaf anatomical characteristics, as there is evidence that soil drought affects both g_m and g_{sc} by changing leaf anatomical characteristics in mesophyll cells and stomata (Chartzoulakis et al., 2002; Tholen et al., 2008; Tosens et al., 2012; Tomás et al., 2013; Xiong et al., 2015a, 2017; Han et al., 2018). First, the surface area of mesophyll cells exposed to intercellular space per unit leaf area (S_{mes}) is thought to be more directly linked to g_m (Evans et al., 1994; Syvertsen et al., 1995; Tomás et al., 2013), as it changes the area of contact between CO_2 and mesophyll cells. Second, the thicknesses of total leaf (T_{leaf}) and mesophyll tissue between the two epidermises (T_{mes}) are found to influence g_m by changing total leaf area (A_T) and mesophyll surface area (A_{mes}), which are the actual areas available for CO_2 diffusion (Niinemets and Reichstein, 2003). Furthermore, the effects of T_{leaf} on g_m and g_{sc} may also result from a change in leaf water supply capacity, as leaf hydraulic conductance (K_{leaf}) had been found to be related to T_{leaf} (Xiong et al., 2015b) and declines in g_m and g_{sc} triggered by leaf hydraulic vulnerability during drought were reported in the study of Wang et al. (2018). Furthermore, as g_m is separated into gas-phase conductance from substomatal cavities to the outer surface of cell walls (g_{ias}) and liquid-phase conductance from the outer surface of cell walls to chloroplasts (g_{liq}) (Evans et al., 1994), the effects of leaf anatomical characteristics on g_m recovery might indirectly result from direct effects on both g_{ias} and g_{liq} (Gillon and Yakir, 2000; Miyazawa et al., 2008a, b). Finally, the g_{sc} recovery is greatly affected by the adjustment of stomatal opening status, as it directly determined the size of the CO_2 diffusion pathway from leaf surface to substomatal cavities (Brodribb and Holbrook, 2004; Brodribb and McAdam, 2011; Ocheltree et al., 2012; Guyot et al., 2012; McAdam and Brodribb, 2013). Thus, adjustments in leaf anatomical characteristics will inevitably have large effects on g_m and g_{sc} recoveries, but it is still unclear whether g_m recovery is mainly driven by leaf g_{ias} or g_{liq}.

In addition, changes in physiological activities might also largely influence the adjustments of leaf anatomical characteristics to a certain extent, as aquaporin (AQP) and carbonic anhydrase (CA) are two key molecules involved in CO_2 and water transmembrane transport. These compounds strongly affect g_m and g_{sc} recoveries by changing their activities (Flexas et al., 2006; Galmés et al., 2007; Mahdieh et al., 2008; Miyazawa et al., 2008a; Uehlein et al., 2008; Sade et al., 2014; Perez-Martin et al., 2014). Miyazawa et al. (2008a) revealed that a decline in AQP activity was a possible reason for a decrease in g_m, which was also supported by the study of Kaldenhoff et al. (2008), who suggested that AQP could regulate the photosynthesis by affecting CO_2 transport from the atmosphere to the chloroplasts through the direct regulation of g_m. Furthermore, Perez-Martin et al. (2014) showed that a decrease in g_m in response to soil drought might be caused by decreased expression of AQP and CA genes and that a decrease in g_m under severe soil drought might be partly due to a decline in CA activity (Flexas et al., 2008, 2012). In addition, changes in AQP and CA activities influence leaf g_{liq}, as they are thought to be two key molecules involved in CO_2 liquid-phase transport (Gillon and Yakir, 2000; Guo et al., 2007; Miyazawa et al., 2008a, b). Thus, AQP and CA greatly adjusted their activities to affect g_m and g_{sc} recoveries, but it was unclear whether these adjustments improved g_m and g_{sc} recoveries in the two species analyzed in the study.

Manchurian ash (*Fraxinus mandshurica* Rupr.) and Mongolian oak (*Quercus mongolica* Fish. ex Ledeb) are two broad-leaved species with different drought tolerances that are well adopted to the typical temperate continental monsoon climate in the Changbai Mountains of Northeast China, which have a cold and long winter and rainy and short summer. However, the responses of g_m and g_{sc} to soil rewatering in both species are poorly understood, and little is known about the recovery mechanisms involving leaf anatomy and physiological activities. To clarify these processes, a rewatering experiment with two initial water stresses (drought before rewatering) was conducted with saplings of both species. The g_m and g_{sc} recoveries, leaf anatomical characteristics and AQP and CA activities were measured. This study aimed to (i) investigate the recoveries of g_m and g_{sc} after different initial water stresses, (ii) explain the mechanisms of g_m and g_{sc} recoveries involving leaf anatomy and physiological activities, and (iii) determine whether g_{ias} or g_{liq} is the main factor promoting g_m recovery.

2. Materials and methods

2.1. Study site

The experiment was conducted at the Research Station of Changbai Mountain Forest Ecosystems of the Chinese Academy of Sciences, located in Jilin Province, Northeast China (128°06′ E, 42°24′ N), at an elevation of 736 m above sea level. The mean annual air temperature in this area is 3.6 °C, and the average annual precipitation is 695 mm. The soil was classified as a typical dark brown forest soil, with concentrations of carbon (C) and nitrogen (N) being 57.24 ± 6.26 and 4.36 ± 0.75 $g\,kg^{-1}$ and C/N ratio being 13.16 ± 0.96, maintaining a higher biological productivity. The main tree species were Manchurian ash (*Fraxinus mandshurica* Rupr.), Mongolian oak (*Quercus mongolica* Fisch. ex Ledeb.), Korean pine (*Pinus koraiensis* Sieb. et Zucc.), *Tilia amurensis* Rupr., *Acer mono* Maxim. and *Betula ermanii* Cham.

2.2. Potted saplings and water control

For each treatment, in April 2015, 5 five-year-old Manchurian ash (*Fraxinus mandshurica* Rupr.) and Mongolian oak (*Quercus mongolica* Fish. ex Ledeb) saplings with similar sizes were planted into 29.28-L pots (30.0-cm height, 34.3-cm diameter) containing 27 l of forest surface soils collected from a broad-leaved Korean pine forest with a field capacity (FC) of 0.426 $g\,cm^{-3}$ (soil volumetric water content, SWC). The pot size was matched to the plant size to avoid unnecessary artifacts in the experiment (Kawaletz et al., 2014). The roots grew spirally around the pots, and pedestals were placed under the pots to prevent roots from protruding into outside soil and to prevent outside water from penetrating the pots. The experiments involved short-term drought followed by rewatering. The water stress intensities were divided into two treatments: medium drought (MW, 40 ± 5% FC) and severe drought (SW, 20 ± 5% FC), with well-watered (90 ± 5% FC) saplings used as the control.

All potted saplings were placed under a 10-m long, 5-m wide and 3.5-m high rain-shelter covered with a transparent plastic film (95% light transmittance), and the rain-shelter was well-ventilated with open sidewalls. The saplings were well irrigated three times per week from budbreak (20 May) to the beginning of the experimental period (20 June) in 2017 to maintain the same growth conditions and then allowed to dry naturally. All saplings were watered in accordance with the requirements of the experimental design beginning on 1 July 2017, and water-stressed saplings were first exposed to drought from the 1st to 20th of each month (named the 'water stress' period) and then rewatered to the level of the controls from the 21st to 30th of the same month (named the 'recovery' period) alternately during July and August in 2017. The control saplings were well irrigated to the FC throughout the study. SWCs (g cm^{-3}) at a 15-cm depth were monitored using a soil humidity real-time observation system (93640Hydra, Stevens, USA) during the water control period, and the data were recorded every half hour. In order to be expressed concisely, the SWC was converted to the relative water content (RWC, RWC = SWC/FC × 100%).

2.3. Pre-dawn leaf water potential measurements

Pre-dawn leaf water potential (Ψ_{pd}, MPa) was measured with a pressure chamber (Model 1505D, PMS Instrument Company, USA) as an indicator of soil moisture stress. Three different leaves were sampled from five replications per treatment before sunrise (06:00), immediately sealed in plastic bags containing a moist towel and kept in a cooler until balancing pressures were completely determined within 1 h after sample collection.

2.4. Simultaneous gas exchange and chlorophyll fluorescence measurements

An open-flow gas exchange system (Li-6400XT; Li-Cor Inc., Lincoln, NE, USA) equipped with an integrated fluorescence leaf chamber (Li-6400-40; Li-Cor) was used to simultaneously measure leaf gas exchange and chlorophyll fluorescence in July and August. To minimize the effects of environments and leaf age, all measurements were conducted on the youngest fully expanded, sun-exposed leaves of five replications from 8:00 to 11:30 each day during measuring periods, with a saturated photosynthetic active photon flux density (PPFD) of 1200 μmol m^{-2} s^{-1} provided by the Li-6400 with a 10 : 90 blue: red light. In the leaf chamber, the leaf temperature was maintained at 25 °C, the relative humidity was approximately 60%, the ambient CO_2 concentration was adjusted to 400 μmol CO_2 mol^{-1} with a CO_2 mixture, and the flow rate was controlled at 300 μmol s^{-1}. The leaves were fully light adapted for 25–30 min before each measurement, and after reaching a steady state, leaf gas exchange parameters, steady-state fluorescence (F_s) and maximum fluorescence (F_m') with a light-saturating pulse of 7800 μmol m^{-2} s^{-1} were recorded using the multiphase flash method (Loriaux et al., 2013). The actual photochemical efficiency of photosystem II ($\Phi_{PS\ II}$) was calculated according to Genty et al. (1989) as follows:

$$\Phi_{PSII} = \frac{(F_m' - F_s)}{F_m'} \tag{1}$$

The electron transport rate (J_f, μmol e^- m^{-2} s^{-1}) was then calculated from formula (2):

$$J_f = \Phi_{PSII} \cdot PPFD \cdot \alpha\beta \tag{2}$$

where α is the total leaf absorptance and β is the partitioning of absorbed quanta between PS II and photosystem I (PS I). In this study, we estimated $\alpha\beta$ from the slope of the relationship between $\Phi_{PS\ II}$ and $4\Phi_{CO2}$ (the quantum efficiency of CO_2 fixation), which were obtained from the light response curves (A_n/PPFD curve) for well-watered, water-stressed and rewatered saplings under a low O_2 concentration (< 1%) achieved by injecting pure N_2 (Valentini et al., 1995; Xiong et al., 2015a).

The chloroplast CO_2 concentration (C_c, μmol CO_2 mol^{-1}) and the g_m were calculated with the 'variable J method' described in Harley et al. (1992):

$$C_c = \frac{\Gamma^*(J_f + 8(A_n + R_d))}{J_f - 4(A_n + R_d)} \tag{3}$$

From Fick's first law of diffusion, g_m was calculated as follows:

$$g_m = \frac{A_n}{(C_i - C_c)} \tag{4}$$

where A_n (μmol CO_2 m^{-2} s^{-1}) is the net photosynthetic rate and C_i (μmol CO_2 mol^{-1}) is the intercellular CO_2 concentration, which were directly obtained from gas exchange measurements; Γ^* (μmol mol^{-1}) represents the CO_2 compensation point in the absence of respiration; and R_d (μmol m^{-2} s^{-1}) represents leaf dark respiration in the light.

Γ^* and R_d were determined using the Laisk method (Laisk, 1977). Namely, three CO_2 response curves were obtained by varying CO_2 concentrations from 150 to 40 μmol CO_2 mol^{-1} under three PPFDs (150, 100 and 50 μmol m^{-2} s^{-1}). The relationship between A_n and C_i under low light and low CO_2 is linear, so these three curves intersected at a point. The intersection point was considered to Γ^* (x-axis) and R_d (y-axis) (Laisk, 1977; von Caemmerer et al., 1994; Pons et al., 2009). Further details of this method can be found in Sun et al. (2015). In this study, Γ^* and R_d were simultaneously measured with gas exchange for controlled, water-stressed and rewatered saplings, and the values were shown in Supplementary Table S1.

In addition, stomatal conductance to CO_2 (g_{sc}, mol CO_2 m^{-2} s^{-1}) was calculated from formula (5):

$$g_{sc} = \frac{g_{sw}}{1.6} \tag{5}$$

where g_{sw} (mol H_2O m^{-2} s^{-1}) is stomatal conductance to water obtained directly from gas exchange measurements and 1.6 is the ratio of the diffusivities of CO_2 and water in air (von Caemmerer and Farquhar, 1981).

2.5. Measurements of leaf anatomical characteristics

Fifteen small leaf samples (4.0 mm × 1.5 mm) were taken from five replications per treatment immediately after leaf gas exchange measurements in July and August and fixed in FAA (alcohol: formaldehyde: glacial acetic acid = 90: 5: 5). Samples were dehydrated in an alcohol series (30% alcohol for 1/2 h, 50% alcohol for 1/2 h, 70% alcohol for 1/2 h, 85% alcohol for 1/2 h, 95% alcohol for 1 h, 100% alcohol for 1 h and 100% alcohol for 1 h) followed by infiltration and finally embedded in Spurr's resin. Semithin leaf cross-sections (8-μm thick) for light microscopy were stained with Saffron-fixing green and then observed at 400 × magnification with a Leica DM2500 light microscope (Leica DM2500, Leica Microsystems GmbH, Wetzlar, Germany).

The thicknesses of leaf (T_{leaf}, μm) and mesophyll tissue (T_{mes}, μm) were measured using Image J software from over 27 horizons. Furthermore, the length of mesophyll cells exposed to intercellular space (L_{mes}, μm) and the cross-sectional width (W, μm) were also measured to calculate the surface area of mesophyll cells exposed to intercellular space per unit leaf area (S_{mes}, $μm^2$ $μm^{-2}$) according to the method in Evans et al. (1994) and Syvertsen et al. (1995):

$$S_{mes} = \frac{L_{mes}}{W} \cdot F \tag{6}$$

where F is the curvature correction factor, which was calculated according to Evans et al. (1994) and Thain (1983). In this study, the F values for controlled, water-stressed and rewatered saplings of both species were shown in Supplementary Table S2.

2.6. Calculations of the gas-phase and liquid-phase conductance

The g_m was a composite conductance with gas-phase conductance from substomatal cavities to the outer surface of cell walls (g_{ias}, m s^{-1}) and liquid-phase conductance from the outer surface of cell walls to chloroplasts (g_{liq}, m s^{-1}) (Evans et al., 1994). g_{ias} was calculated according to the description in Niinemets and Reichstein (2003):

$$g_{ias} = \frac{D_a f_{ias}}{\Delta L_{ias} \zeta} \tag{7}$$

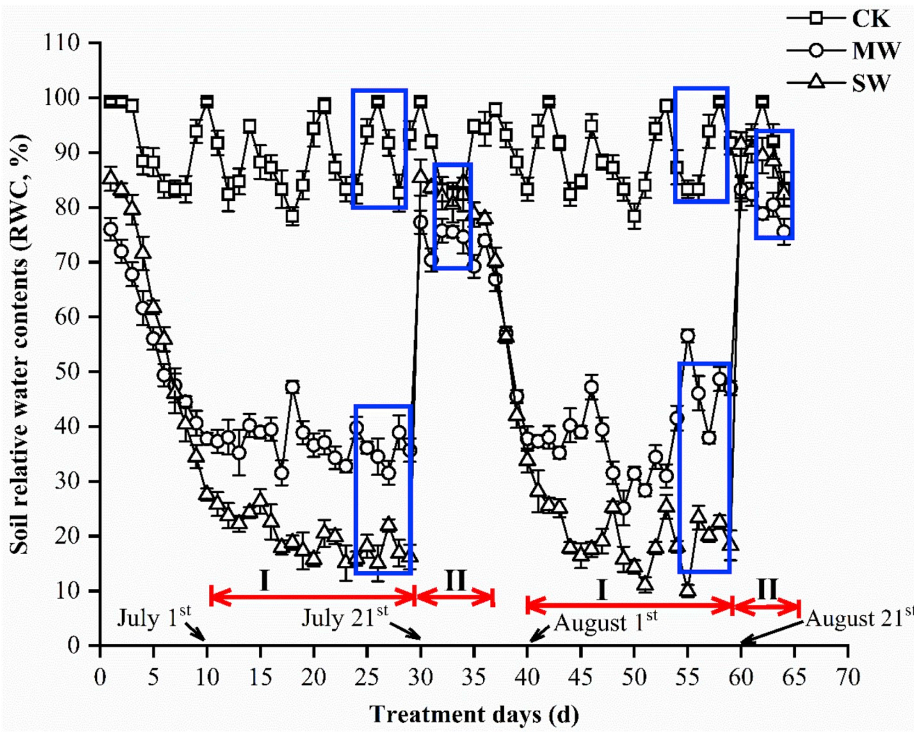

Fig. 1. Variations of daily soil relative water contents (RWC, %) during water stress (I) and re-watering (II) in July and August. All data were the averages of both species' pots with variations (n = 3). CK, control; MW, medium water stress; SW, severe water stress. Gas exchange measuring and leaf sampling were performed in the days marked with blue box. (For interpretation of the references to color in this figure legend, the reader is referred to the Web version of this article.)

where D_a ($m^2 s^{-1}$) is the diffusion coefficient for CO_2 in the gas phase (1.51×10^{-5} at 25 °C) (Tomás et al., 2013). ΔL_{ias} (μm) was taken as half T_{mes} (Niinemets and Reichstein, 2003). ς is the diffusion path tortuosity ($m\ m^{-1}$), which was valued at 1.57 (Syvertsen et al., 1995; Niinemets and Reichstein, 2003). f_{ias} (%) is the fraction of mesophyll volume occupied by the intercellular airspace, which was calculated according to the description in the study of Syvertsen et al. (1995).

The g_{liq} was provided by the sum of the inverses of serial conductance (Niinemets and Reichstein, 2003; Tosens et al., 2016):

$$\frac{1}{g_{liq}} = \left(\frac{1}{g_{cw}} + \frac{1}{g_{pl}} + \frac{1}{g_{ct}} + \frac{1}{g_{en}} + \frac{1}{g_{st}}\right)\frac{A_T}{A_{mes}} \tag{8}$$

where g_{cw}, g_{pl}, g_{ct}, g_{en} and g_{st} are the partial conductance for the cell wall, plasmalemma, cytosol, chloroplast envelope and chloroplast stroma ($m\ s^{-1}$), respectively. g_{cw}, g_{ct} and g_{st} were calculated as described in Niinemets and Reichstein (2003), while g_{pl} and g_{en} were estimated to be $0.0035\ m\ s^{-1}$, as suggested in previous studies (Evans et al., 1994; Tosens et al., 2012). Mesophyll surface area (A_{mes}, μm^2) and total leaf surface area (A_T, μm^2) corrected for the actual area available for CO_2 diffusions were also measured using Image J software.

2.7. Measurements of stomatal opening status

Small leaf samples (4.0 mm × 1.5 mm) were fixed in 2.5% glutaraldehyde in 0.1 M phosphate buffer (pH = 7.6) at 4 °C and then stored at 4 °C until further treatment. The saplings were flushed 2–3 times with phosphate buffer (pH = 7.6) and dehydrated with a gradient of 50%, 70%, 90% and 100% ethanol for 5–10 min at each concentration. Then, alcohol-tert-butyl alcohol solution (1:1, v/v) was used to exchange them for 20 min, and 100% tert-butyl alcohol was used to exchange them twice, for 20 min each time. Finally, leaf samples were freeze dried for 1–2 h with tert-butyl alcohol. Nine images of the abaxial and adaxial epidermal surfaces of each leaf were captured under a vacuum with an environmental scanning electron microscope (Quanta-250, FEI company, USA). Stomatal pore length (PL, μm) and width (PW, μm) at the center of the stoma were measured using Image J software to calculate the stomatal pore size (SS, μm^2) (Xiong et al., 2017). In this study, the SS was calculated based on the assumption that the stomatal pore is an ellipse with a major axis equal to PL and a minor axis equal to PW, following formula (9):

$$\text{Stomatal pore size (SS)} = \frac{\pi \cdot PL \cdot PW}{4} \tag{9}$$

2.8. Measurements of leaf AQP and CA activities

Fifteen fresh leaves per treatment were sampled to measure AQP and CA activities using the enzyme-linked immunosorbent assay (ELISA) according to Maeda et al. (1995). Purified plant AQP (or CA) antibody was used to coat microtiter plate wells and make solid-phase antibody; then, AQP (or CA) were added to wells. A combined antibody labelled with horseradish peroxidase (HRP) became an antibody-antigen-enzyme-antibody complex, and 3,3′,5,5′-tetramethyl benzidine (TMB) substrate solution was then added for color after complete washing. Catalyzed by the HRP enzyme, the TMB substrate became blue, and the reaction was terminated by the addition of a sulfuric acid solution. The color change was measured spectrophotometrically at a wavelength of 450 nm. The activities of AQP and CA in the samples were determined by comparing the optical density (OD) values of the samples to the standard curves.

2.9. Statistical analysis

A one-way analysis of normality and homogeneity of variance between treatments in g_m, g_{sc}, A_n, leaf anatomical characteristics and both activities of AQP and CA was performed using SPSS 17.0 (SPSS Inc., Chicago, IL, USA). Furthermore, the regression analyses between g_m and g_{ias} & g_{liq} were also performed. Mean values were compared using a least significant difference (LSD) multiple comparison test at the 0.05 probability level ($P < 0.05$) with Tukey's honest significant difference (HSD) test. The data in two stages of pre-drought (initial drought) and rewatering were mixed analyzed to compare the differences between soil drought and rewatering to further highlight the effects of re-watering.

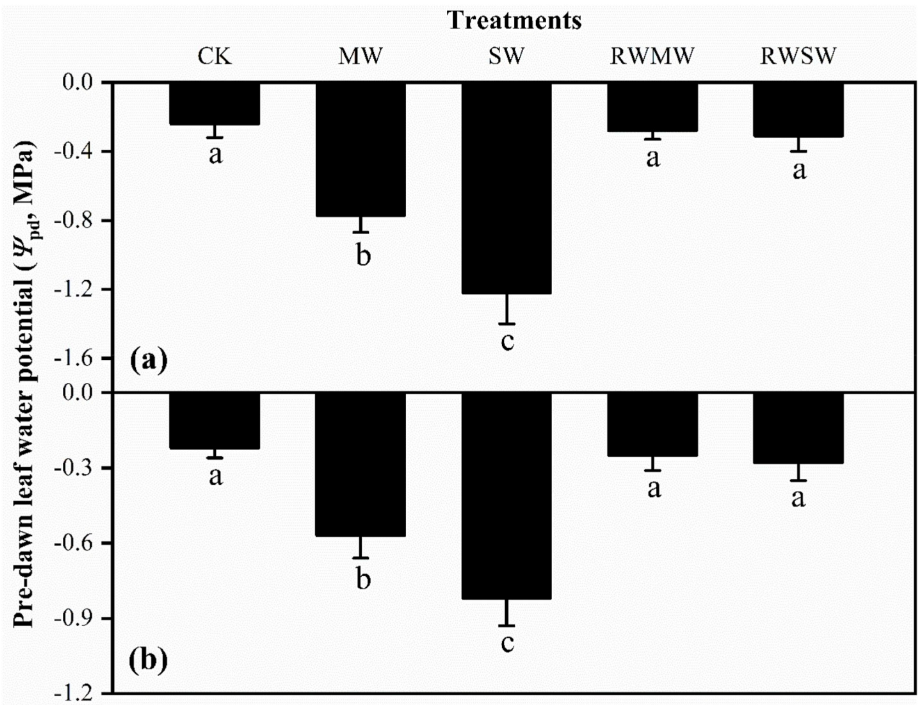

Fig. 2. Pre-dawn leaf water potential (Ψ_{pd}, MPa) responses to different treatments for Manchurian ash (a) and Mongolian oak (b) (n = 3). The error bar represents standard error of all measurements in each individual tree species (The same in below.). Different letters indicate significant difference among each group treatments ($P < 0.05$). CK, the control; MW, medium water stress; SW, severe water stress; RWMW, rewatering after initial medium water stress; RWSW, rewatering after initial severe water stress.

3. Results

3.1. Variations in daily soil RWCs and pre-dawn leaf water potential

Fig. 1 shows the variations in daily RWCs under three water control levels (well-watered, water-stressed and rewatered) together with the rewatering date and water control periods (‘water stress’ period and ‘recovery’ period). The RWC in well-watered pots (control, CK) fluctuated somewhat, varying from 78.4 to 99.3%, while the RWC in the water-stressed pots decreased significantly from approximate 80% at the beginning of the treatment to 37.8% (MW) and 27.6% (SW) after water stress began on 1 July. During the water stress periods (I), the RWC in the MW and SW treatments was maintained at an average of 38.0 ± 5.9% and 20.5 ± 5.4%, respectively. After rewatering on 1 July and 1 August (II), the RWC were fully recovered to the control level.

We also measured pre-dawn leaf water potential (Ψ_{pd}) as an indicator of soil moisture stress (Fig. 2). The mean Ψ_{pd} in the CK treatment was −0.24 ± 0.08 MPa, which decreased to −0.77 ± 0.10 and −1.22 ± 0.18 MPa in the MW and SW treatments for Manchurian ash saplings, respectively, and to −0.57 ± 0.09 (MW) and −0.82 ± 0.11 MPa (SW) for Mongolian oak saplings. After rewatering, leaf Ψ_{pd} increased to −0.28 ± 0.05 (MW) and −0.31 ± 0.09 MPa (SW) for Manchurian ash saplings and to −0.25 ± 0.06 (MW) and −0.28 ± 0.07 MPa (SW) for Mongolian oak saplings.

3.2. Changes in both g_m and g_{sc} during water stress

Fig. 3-I and II show the changes in g_m, g_{sc} and A_n for both species during water stress in July and August. Both species (Manchurian ash and Mongolian oak) showed a decline in g_m and g_{sc} as soil water availability decreased, and significant differences were detected in overall among the water stress treatments ($P < 0.05$). g_m and g_{sc} decreased by 31.2% and 22.6% (MW) and 52.4% and 32.2% (SW) in July and by 48.2% and 15.6% (MW) and 63.0% and 30.2% (SW) in August for Manchurian ash saplings and by 26.2% and 45.8% (MW) and 54.0% and 62.1% (SW) in July and 34.6% and 50.4% (MW) and 61.4% and 71.3% (SW) in August for Mongolian oak saplings, respectively, compared with the controls. g_m decreased more than g_{sc} in Manchurian ash, while g_{sc} decreased much more in Mongolian oak saplings. Affected by the g_m and g_{sc} declines, A_n decreased by 34.0% (MW) and 44.1% (SW) in July and 32.8% (MW) and 46.2% (SW) in August in Manchurian ash saplings and by 45.1% (MW) and 75.0% (SW) in July and 46.3% (MW) and 66.2% (SW) in August in Mongolian oak saplings.

3.3. Effects of rewatering on g_m and g_{sc}

3.3.1. Difference in g_m and g_{sc} recoveries between Manchurian ash and Mongolian oak

The changes in g_m, g_{sc} and A_n after rewatering for both species are also shown in Fig. 3-I and II, which reveal that rewatering made a recovery effect on both g_m and g_{sc} but that this effect differed between Manchurian ash and Mongolian oak. For Manchurian ash, g_m recovered to 85.9% (MW) and 68.9% (SW) of that in the controls in July and to 72.9% (MW) and 56.9% (SW) in August, while g_{sc} recovered to 87.2% (MW) and 78.5% (SW) in July and to 92.1% (MW) and 82.9% (SW) in August. For Mongolian oak, g_m recovered to 88.8% (MW) and 68.0% (SW) of that in the controls in July and to 81.2% (MW) and 60.0% (SW) in August, while g_{sc} recovered to 70.8% (MW) and 47.8% (SW) in July and to 68.3% (MW) and 54.1% (SW) in August. The g_m recovered much more in Mongolian oak, while Manchurian ash displayed a larger recovery in g_{sc}. Furthermore, the recoveries did not differ significantly between July and August. Promoted by the g_m and g_{sc} recoveries, A_n recovered to apporoximately 82.7% (MW) and 68.9% (SW) of that in the controls for both species.

3.3.2. Recoveries of g_m and g_{sc} after different initial water stresses

The recoveries of g_m and g_{sc} also depended somewhat on the initial water control levels (Fig. 3-I and II). In the initial MW treatment, g_m recovered by an average of 49.2% (Manchurian ash) and 51.5% (Mongolian oak) more than that in the initial severe water stress (SW) treatment, while g_{sc} recovered by 46.2% (Manchurian ash) and 36.6% (Mongolian oak) more. Both g_m and g_{sc} recovered much more in the initial MW treatment; in other words, the recoveries of g_m and g_{sc} declined with initial water stress.

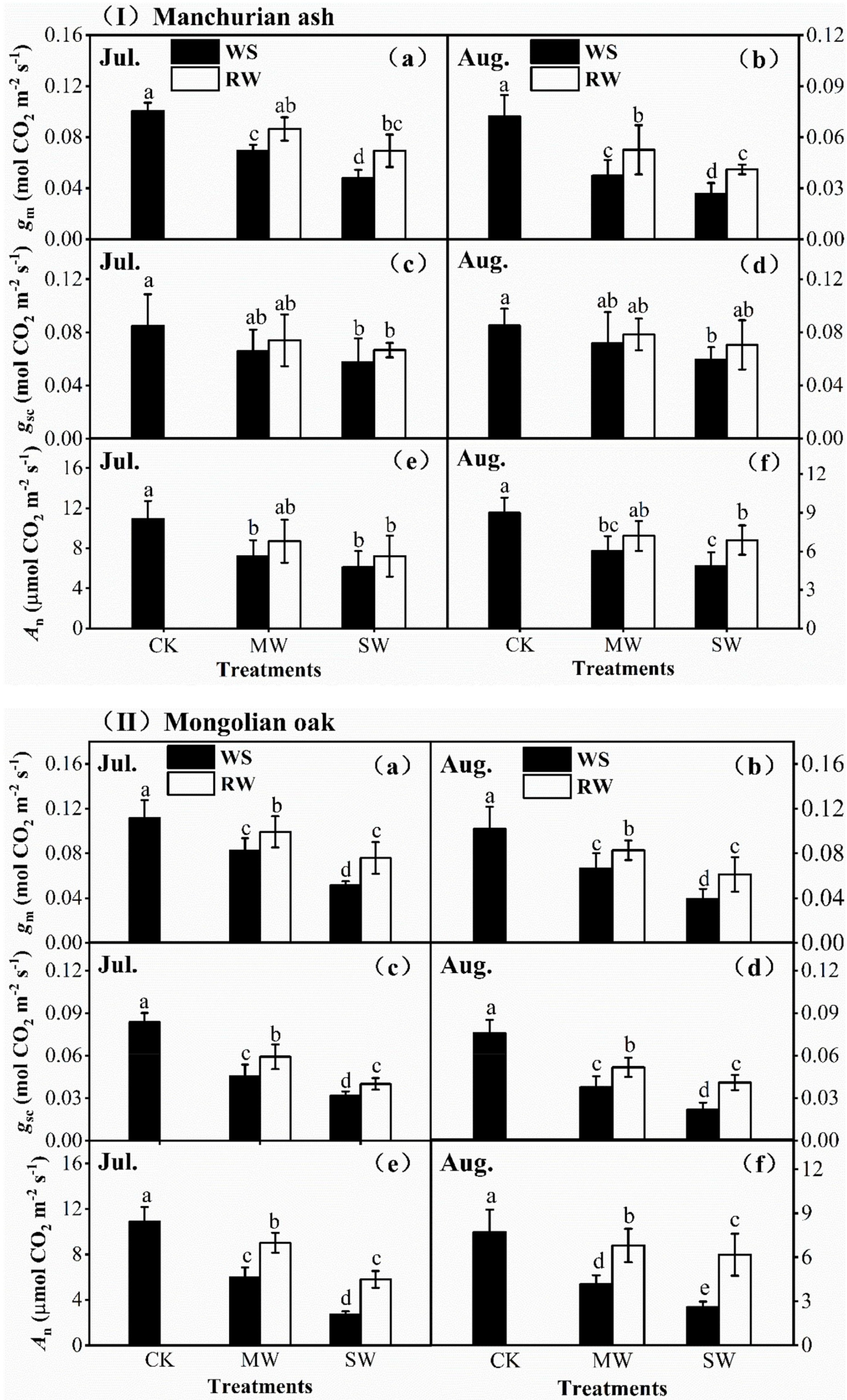

Fig. 3. Changes of g_m, g_{sc} and A_n during water stress and rewatering for Manchurian ash (I) and Mongolian oak saplings (II). Values are means ± SE (n = 5), and different lowercase letters (a, b, c) indicate significant difference at $P < 0.05$. CK, control; MW, medium water stress; SW, severe water stress. WS, water stress treatment; RW, rewatering treatment.

3.4. Adjustments in leaf anatomy

3.4.1. Changes in mesophyll cell morphologies

Light micrographs of leaf transverse sections showed a significant difference before and after rewatering (Fig. 4). Compared with the control, water-stressed saplings showed a shriveled leaf anatomical structure. Mesophyll cells adhered to form many clusters, and this clustering was aggravated by water stress (Fig. 4-b, d, g and i).

After rewatering, with the recovery of soil water contents, mesophyll cells gradually swelled and adherence-relieved, in turn reconnecting to each other (Fig. 4-c, e, h and j). Furthermore, both length and width of palisade and spongy tissues increased after rewatering,

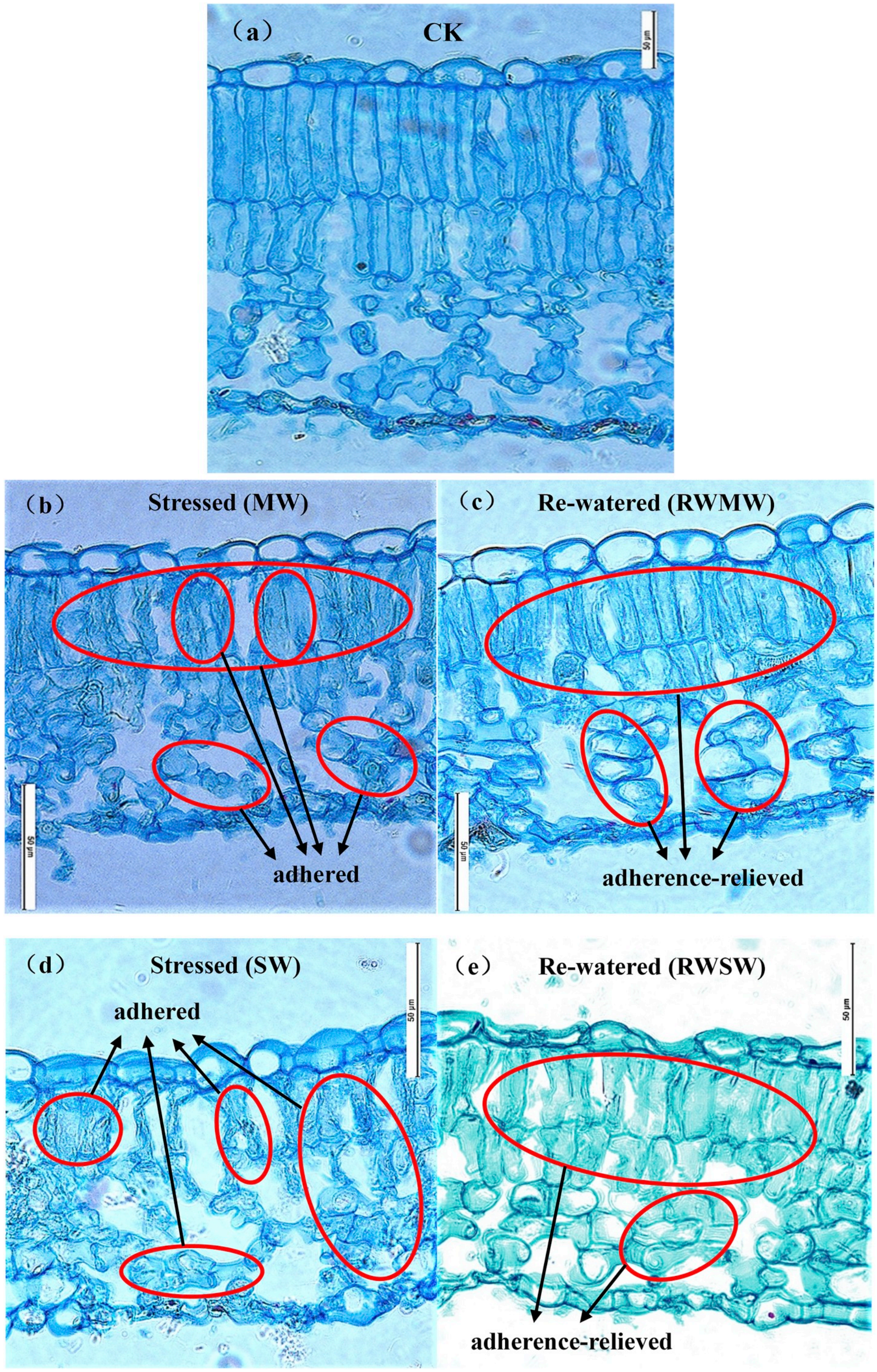

Fig. 4. Light micrographs of transverse sections for controlled, water-stressed and re-watered leaves for Manchurian ash (a–e) and Mongolian oak saplings (f–j). Scale bar = 50 μm. All leaf cross-sections were observed at 400 × magnification, but for better observation, some anatomical micrographs were enlarged. Red circles represent palisade and spongy tissues "adhered together (Stressed)" and "adherence-relieved to each other (Recovery)". CK, the control; MW, medium water stress; SW, severe water stress; RWMW, rewatering after initial medium water stress; RWSW, rewatering after initial severe water stress. (For interpretation of the references to color in this figure legend, the reader is referred to the Web version of this article.)

suggesting an enlarged surface area of mesophyll cells. All these changes in mesophyll cell morphologies would inevitably change the CO_2 diffusion pathways.

3.4.2. Changes in mesophyll anatomical characteristics

The changes in mesophyll cell morphologies led to different responses of leaf anatomical characteristics to soil water stress and rewatering (Table 1). Both T_{leaf} and T_{mes} significantly decreased with water stress in both species ($P < 0.05$). In addition, the adherences of palisade and spongy tissues during water stress directly decreased S_{mes} by 19.5% (MW) and 21.1% (SW) relative to the control values for Manchurian ash saplings and by 20.5% (MW) and 24.1% (SW) for Mongolian oak saplings, respectively, and no statistically significant difference was found between the MW and SW treatments ($P < 0.05$).

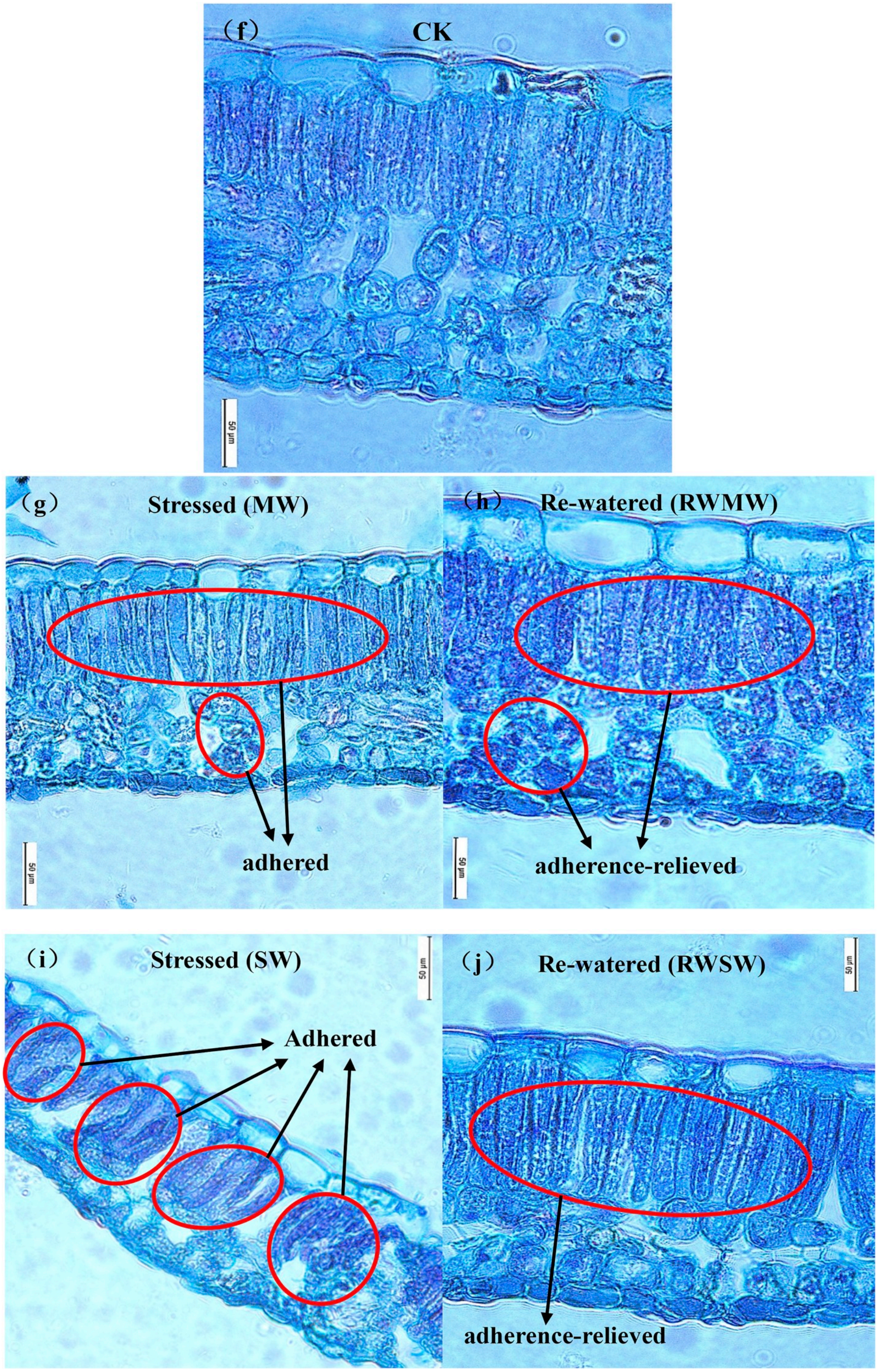

Fig. 4. (*continued*)

After rewatering, both T_{leaf} and T_{mes} increased significantly, but S_{mes} decreased by 0.6% (MW) and 23.1 (SW) in Manchurian ash saplings and by 2.9% (MW) and 10.3% (SW) in Mongolian oak saplings, respectively, on the basis of stressed values, even showing a significant difference before and after rewatering in the initial SW treatment ($P < 0.05$).

3.4.3. Changes in leaf g_{ias} and g_{liq}

The changes in mesophyll anatomical characteristics caused different responses of g_{ias} and g_{liq} to water stress and rewatering (Table 1). g_{ias} increased with water stress and decreased after rewatering, showing a pattern in contrast to that of g_m, but no statistically significant differences were detected in overall among the treatments ($P < 0.05$). Changes in both T_{leaf} and T_{mes} led to an increase in the A_T/A_{mes} ratio during the period of soil drought and a decrease after rewatering, which directly caused the g_{liq} to decrease with water stress and markedly increase after rewatering. Furthermore, g_{liq} differed significantly before and after rewatering in both species ($P < 0.05$).

3.4.4. Changes in SS

Table 2 shows the values of stomatal features for both species during water stress and rewatering. SS, including PL and PW at the center of the stoma, contrasted considerably during water stress and after rewatering. With a decreasing soil water contents, both PL and PW

Table 1
Values of leaf anatomical characteristics for controlled, water-stressed and re-watered saplings during water stress and rewatering for both species.

	Manchurian ash						Mongolian oak					
	Tleaf (µm)	Tmes (µm	Smes (µm2 µm-2)	AT/Ames	gias (10-2 m s-1)	gliq (10-4 m s-1)	Tleaf (µm)	Tmes (µm)	Smes (µm2 µm-2)	AT/Ames	gias (10-2 m s-1)	gliq (10-4 m s-1)
CK	130.1 ± 11.0^{a}	116.3 ± 5.1^{a}	12.1 ± 2.0^{a}	1.91 ± 0.08^{b}	4.47 ± 0.37^{b}	1.08 ± 0.06^{b}	206.8 ± 3.2^{c}	158.1 ± 6.7^{c}	12.9 ± 1.3^{a}	1.81 ± 0.11^{c}	5.41 ± 0.33^{b}	1.14 ± 0.06^{a}
MW	112.3 ± 1.1^{b}	95.6 ± 1.8^{c}	9.7 ± 0.6^{b}	2.08 ± 0.13^{ab}	5.55 ± 0.53^{b}	0.99 ± 0.04^{b}	180.1 ± 1.9^{d}	145.3 ± 5.0^{d}	10.3 ± 0.5^{b}	2.56 ± 0.34^{b}	5.93 ± 0.22^{a}	0.81 ± 0.02^{c}
SW	101.2 ± 1.7^{c}	82.9 ± 1.7^{e}	9.5 ± 0.8^{b}	2.43 ± 0.47^{a}	10.19 ± 1.74^{a}	0.85 ± 0.06^{c}	126.7 ± 8.5^{e}	95.0 ± 7.5^{e}	9.8 ± 0.2^{b}	3.90 ± 0.30^{a}	5.53 ± 0.24^{ab}	0.53 ± 0.01^{d}
RWMW	124.6 ± 2.4^{a}	105.9 ± 1.2^{b}	9.7 ± 1.5^{b}	1.92 ± 0.04^{b}	5.26 ± 0.41^{b}	1.08 ± 0.05^{b}	235.4 ± 4.5^{a}	183.6 ± 2.4^{b}	10.0 ± 1.7^{b}	1.96 ± 0.09^{c}	5.51 ± 0.30^{ab}	1.06 ± 0.04^{b}
RWSW	110.9 ± 3.6^{bc}	89.2 ± 1.6^{d}	7.3 ± 1.0^{c}	1.70 ± 0.06^{b}	9.75 ± 0.33^{a}	1.22 ± 0.04^{a}	226.3 ± 4.3^{b}	196.6 ± 6.6^{a}	8.8 ± 0.7^{c}	1.84 ± 0.06^{c}	4.90 ± 0.20^{c}	1.13 ± 0.05^{ab}

All data were means ± SE (n = 5). Different lowercase letters (a, b, c) indicate significant differences at $P < 0.05$. T_{leaf}, total leaf thickness; T_{mes}, mesophyll tissue thickness between the two epidermises; S_{mes}, the surface area of mesophyll cells exposed to intercellular space per unit leaf area; A_T/A_{mes}, the ratio of mesophyll surface (A_{mes}) to total leaf surface area (A_T) corrects for the actual area available for CO_2 diffusion; g_{ias}, CO_2 gas-phase conductance from sub-stomatal cavities to outer surface of cell walls; g_{liq}, CO_2 liquid-phase conductance from outer surface of cell walls to chloroplasts. CK, the control; MW, medium water stress; SW, severe water stress; RWMW, rewatering after initial medium water stress; RWSW, rewatering after initial severe water stress.

decreased and directly caused a significant decline in SS of approximately 8 µm^2 for Manchurian ash saplings and approximately 2 µm^2 for Mongolian oak saplings ($P < 0.05$), which might have been caused by the shrinkage of guard cells. After rewatering, both PL and PW increased, which also caused a significant increase in SS of approximately 4 µm^2 for Manchurian ash saplings and approximately 2 µm^2 for Mongolian oak saplings compared with that before rewatering ($P < 0.05$), and the more serious the initial water stress was, the higher the recovery. The recovery of SS increased the stomatal opening status and promoted the recovery of g_{sc}.

3.5. Changes in leaf AQP and CA activities

Table 3 shows the values of leaf AQP and CA activities for both species during water stress and rewatering. The AQP and CA activities for both species decreased with water stress but increased after rewatering. Overall, there was a significant difference between treatments ($P < 0.05$). In addition, both activities of AQP and CA in the SW treatment were lower than those in the MW treatment, and this was not changed by soil rewatering. The decrease in AQP activity weakened the transmembrane transport of CO_2, and the transmission of CO_2 to $-HCO_3$ was also weakened with a decrease in CA activity. Soil rewatering increased the activities of AQP and CA, thereby strengthening the transmembrane transport of CO_2 and water and promoting the expression of AQP and CA genes, further increasing g_m and g_{sc}.

4. Discussion

4.1. Recoveries of g_m and g_{sc} after rewatering

Rewatering led to the recoveries of both g_m and g_{sc}, which had been reported by earlier studies (Galmés et al., 2007; Galle et al., 2009; Flexas et al., 2009; Cano et al., 2014; Cai et al., 2015). In this study, the recoveries of g_m and g_{sc} varied from 47.8% to 92.1% in July and August in both species, being a moderate level among relative researches in overall, which are slightly higher than those in the study of Perez-Martin et al. (2014) that the g_m of *Olea europaea* L. var. Manzanilla plants recovered by 35–53% and g_{sc} recovered by only 6–35% after 4 days of rewatering, but markedly lower than the studies of Galmés et al. (2007) and Galle et al. (2007) that both g_m and g_{sc} were completely recovered after 1–3 days of rewatering. Besides, our data showed that g_m and g_{sc} made different recoveries to soil rewatering, in which g_m recovered much more in Mongolian oak while g_{sc} recovered more in Manchurian ash. This was agreed with the studies of Flexas et al. (2009) on *Vitis berlandieri* × *Vitis rupestris* and Cai et al. (2015) on *Rhododendron delavayi* Franch., in which g_m was completely recovered but g_{sc} made no significant recovery in the former species or recovered to only 70–86% in the later species. Furthermore, Cai et al. (2015) found that with further recovery of g_{sc} after 3 days of rewatering, g_m was no longer restored and even slightly decreased.

We also explored the effects of different initial water stresses on g_m and g_{sc} recoveries in this study and found a larger recovery of g_m and g_{sc} after the initial medium water stress treatment. This might be because the saplings in the initial medium water stress treatment were less damaged than those in the initial severe water stress treatment and maintained a better recovery capacity (Kunz et al., 2016). Therefore, the recoveries of g_m and g_{sc} were also related to the initial water stress conditions.

The recoveries of g_m and g_{sc} greatly promoted A_n recovery, but this promotion was species dependent, as the g_m and g_{sc} recoveries showed some species dependence in this study. The recovery of A_n in Manchurian ash was mostly affected by g_{sc} recovery, as g_{sc} recovered much more after rewatering than g_m, while the recovery of A_n in Mongolian oak was strongly promoted by the greater recovery of g_m. This difference in the driver of A_n recovery might be related to the different drought tolerances of the species. Manchurian ash is a water-

Table 2
Values of stomatal pore size (SS), including stoma pore length (PL) and pore width (PW) at the center of the stoma for controlled (CK), water-stressed and re-watered leaves for both species.

	Manchurian ash			Mongolian oak		
	PL (μm)	PW (μm)	SS (μm^2)	PL (μm)	PW (μm)	SS (μm^2)
CK	7.01 ± 0.70^a	3.04 ± 0.97^a	17.57 ± 1.72^a	6.36 ± 0.52^a	2.47 ± 0.58^a	12.78 ± 1.15^a
MW	5.08 ± 0.36^{bc}	2.60 ± 0.90^a	10.98 ± 1.47^c	6.16 ± 0. 47^a	2.28 ± 0.53^a	11.40 ± 1.19^{ab}
SW	4.05 ± 0.21^c	2.17 ± 0.32^a	6.95 ± 1.37^d	5.42 ± 0.80^a	2.14 ± 0.67^a	9.52 ± 1.90^b
RWMW	6.71 ± 0.17^a	2.77 ± 0.49^a	14.76 ± 2.63^{ab}	6.22 ± 0.76^a	2.59 ± 0.58^a	12.91 ± 1.56^a
RWSW	5.58 ± 0.98^b	2.33 ± 0.94^a	11.20 ± 2.64^{bc}	6.23 ± 0.80^a	2.60 ± 0.44^a	12.96 ± 1.74^a

All data were means ± SE (n = 64). Different lowercase letters (a, b, c) indicate significant differences at $P < 0.05$. CK, the control; MW, medium water stress; SW, severe water stress; RWMW, rewatering after initial medium water stress; RWSW, rewatering after initial severe water stress.

Table 3
Values of leaf aquaporin (AQP) and carbonic anhydrase (CA) activities for controlled, water-stressed and re-watered saplings during water stress and re-watering for both species.

	Manchurian ash		Mongolian oak	
	AQP (U g^{-1})	CA (U g^{-1})	AQP (U g^{-1})	CA (U g^{-1})
CK	5.57 ± 0.29^a	1.54 ± 0.09^a	5.57 ± 0.15^a	1.42 ± 0.10^a
MW	4.90 ± 0.36^{bc}	1.07 ± 0.05^d	4.86 ± 0.09^{bc}	1.19 ± 0.07^b
SW	4.45 ± 0.13^d	0.79 ± 0.02^e	4.03 ± 0.08^d	1.01 ± 0.02^c
RWMW	5.01 ± 0.09^b	1.39 ± 0.21^b	4.98 ± 0.08^b	1.25 ± 0.09^b
RWSW	4.67 ± 0.29^{cd}	1.27 ± 0.05^c	4.70 ± 0.22^c	1.15 ± 0.06^b

All data were means ± SE (n = 5). Different lowercase letters (a, b, c) indicate significant differences among treatments at $P < 0.05$. CK, the control; MW, medium water stress; SW, severe water stress; RWMW, rewatering after initial medium water stress; RWSW, rewatering after initial severe water stress.

loving species and is more sensitive to changes in soil moisture content, while Mongolian oak has a stronger drought tolerance and is slightly influenced by the alternation of drought and rewatering. However, our results partly differ from the results of Cai et al. (2015), who showed that g_m rather than g_{sc} or other biochemical factors had the most important effect on photosynthesis recovery, which was also suggested in the study of Galmés et al. (2007), in which g_m recovery was the driver of photosynthetic recovery of severely stressed plants after rewatering.

However, the present results might not completely reflect the mature trees' responses to soil drought and rewatering. Samuelson and Michael Kelly, 2001 suggested that variation in stomatal conductance to water vapor (g_{sw}) might be different in saplings and mature trees responding to soil water availability. In addition, the variation in foliar N concentration between saplings and mature trees could also result in the differences in leaf gas-exchange rates (Samuelson and Michael Kelly, 2001), since photosynthetic capacity was often positively correlated with foliar nitrogen (N) concentration (Field and Mooney, 1986). Furthermore, Niinemets (2010) suggested that tree tolerance to many environmental stresses such as drought increases throughout the ontogeny as the result of accumulation of non-structural carbon pools. Hence, considering the mature trees had much stronger drought tolerance and higher foliar N concentrations in general (Fredericksen et al., 1995, 1996; Kolb et al., 1997; Cavender-Bares and Bazzaz, 2000; Fleischmann et al., 2005, 2009; Nunn et al., 2005; Tu et al., 2016), mature trees in Manchurian ash and Mongolian oak might maintain a slighter decline in g_m and g_{sc} during soil drought, and might also have a larger even complete recovery in mesophyll and stomatal conductance after rewatering.

4.2. Mechanisms of g_m and g_{sc} recoveries involving leaf anatomy

In this study, leaf cross-sections from stressed saplings revealed that both palisade and spongy tissues adhered together to form clusters during water stress, in turn increasing the chlorenchyma cell density and increasing the difficulty of CO_2 diffusion through mesophyll cells to the site of chloroplast carboxylation (Chartzoulakis et al., 2002), but this status was relieved by soil rewatering. After rewatering, the predawn leaf water potential (Ψ_{pd}) increased (Fig. 2), the adherence of palisade and spongy tissues was relieved, and mesophyll cells were reconnected to each other, which not only decreased CO_2 diffusional difficulties but also improved the contact areas between palisade and spongy tissues, thus increasing g_m.

Compared with the qualitative descriptions of mesophyll cell morphologies, the quantitative changes in leaf anatomical characteristics provided a clearer mechanism of g_m recovery. First, S_{mes} decreased with water stress and after rewatering (Table 1), showing responses partially similar to those of g_m. Hence, S_{mes} had a negative effect on g_m recovery. Second, both T_{leaf} and T_{mes} increased after rewatering in this study (Table 1); these increases not only enlarged total leaf and mesophyll surface areas for the actual areas available for CO_2 diffusion (Niinemets and Reichstein, 2003), but also widened CO_2 flow pathways, as thicker leaves have more parallel flow pathways outside the xylem (Xiong et al., 2015b). Thus, the negative effects of the S_{mes} decrease on g_m recovery might be largely compensated for by the large increases in T_{leaf} and T_{mes}. In addition, the g_m recovery might also be greatly promoted by an increase in the chloroplast surface facing the intercellular space per unit leaf area (S_c) (Evans et al., 2009; Tosens et al., 2012, 2016; Tomás et al., 2013; Xiong et al., 2017), as S_c was suggested to be tightly related to mesophyll cells, the shapes of chloroplasts and the light-dependent arrangement of chloroplasts (Tholen et al., 2008) and might have a positive effect on g_m recovery, although S_c was not measured in this study.

Furthermore, leaf anatomical characteristics may indirectly affect g_m recovery by directly affecting g_{ias} and g_{liq}, which compose g_m (Evans et al., 1994). In this study, g_{ias} increased with water stress and decreased after rewatering, while g_{liq} exhibited responses to water stress and rewatering identical to those of g_m (Table 1). Hence, the increases in leaf anatomical characteristics significantly promoted the CO_2 liquid-phase transport process but suppressed gas-phase transport, and the g_m recovery might be mainly promoted by g_{liq} rather than by g_{ias}. This was also strongly supported by the contrary relationships of g_{ias} and g_{liq} with g_m, in which g_m was negatively correlated with g_{ias} but positively correlated with g_{liq} in both species (Fig. 5). Our result agreed with that in the study of Evans et al. (1994), who concluded that g_{ias} was not a major determinant of g_m in leaves. Furthermore, our result was also indirectly supported by the study of Miyazawa et al. (2008a), who attributed a significant reduction in g_m to a decrease in g_{liq}. Consequently, the g_m recovery in both species should mainly result from the great increase in g_{liq} after rewatering rather than that in g_{ias}.

Compared with the complex mechanisms of g_m recovery, those of g_{sc} recovery were relatively clear. Based on the suggestion of Xiong et al. (2017) that g_{sc} was determined by both stomatal size and opening status, the increase in SS after rewatering induced by increases in the stomatal PL and PW at the center of the stoma increases in this study greatly improved stomatal opening status (Table 2), which

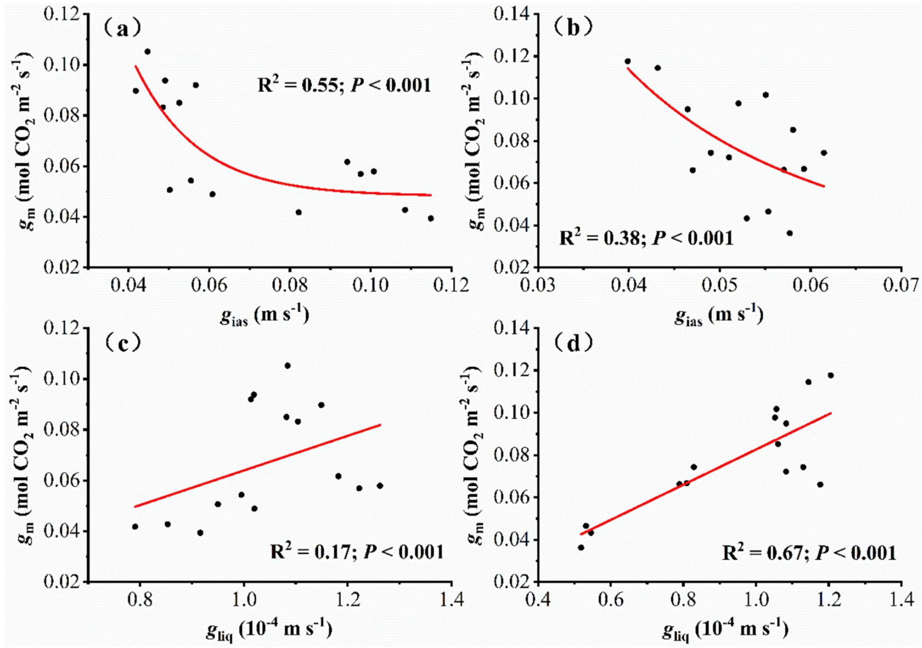

Fig. 5. The correlations between g_m and g_{ias} & g_{liq} for Manchurian ash (a, c) and Mongolian oak saplings (b, d) in this study.

strengthened CO_2 diffusion from leaf surface to substomatal cavities and then significantly promoted g_{sc} recovery, consistent with findings from the study of Ocheltree et al. (2012).

4.3. Mechanisms of g_m and g_{sc} recoveries involving AQP and CA activities

As discussed above, the g_m recovery should be mainly due to the great increase in g_{liq} after rewatering, and g_{liq} has already been suggested to be related to AQP and CA activities (Gillon and Yakir, 2000; Guo et al., 2007; Miyazawa et al., 2008a, b). Hence, the increase in g_{liq} might be largely promoted by the increases in AQP and CA activities in both species, which was strongly supported by our result. In this study, the activities of both AQP and CA decreased with water stress, while they increased after rewatering (Table 3) and were positively correlated with g_m. Since g_{liq} is the capacity for CO_2 transmembrane transport among the cell wall, cytosol, chloroplast envelope and chloroplast stroma (Evans et al., 1994), the increases in AQP and CA activities significantly improved these capacities, as AQP has been found to be water and CO_2 channels in many plant species such as *Hordeum vulgare* L. (Mori et al., 2014), rice (Hanba et al., 2004) and *Arabidopsis thaliana* (Heckwolf et al., 2011), while CA has been suggested to regulate g_m by changing the dynamics of CO_2 and $-HCO_3$ (Gillon and Yakir, 2000; Perez-Martin et al., 2014). The promotions of AQP and CA activities leading to increases in g_m and g_{sc} recoveries might be explained by the following three aspects.

First, the increase in AQP activity might strongly promote the expression of genes in the plasma membrane intrinsic proteins (PIPs) aquaporin family, mediated by AQP, and then improve CO_2 and water membrane permeabilities via AQP in both species (Uehlein et al., 2003; Flexas et al., 2006; Perez-Martin et al., 2011). Such a process directly improves CO_2 transmembrane transport and consequently increases both g_m and g_{sc} (Hanba et al., 2004; Flexas et al., 2006; Perez-Martin et al., 2014; Xiong et al., 2015a; Han et al., 2018). Second, the increase in CA activity would greatly strengthen the transmission of CO_2 to $-HCO_3$ and then promote CO_2 diffusion, further increasing both g_m and g_{sc}. Third, the positive effects of AQP and CA activities on g_m and g_{sc} recoveries might be largely promoted by leaf anatomical structure adjustments. The adherence between mesophyll tissues was relieved after rewatering, which reconnected mesophyll cells to each other and enlarged the areas of contact between cells (Fig. 4). CO_2 transmembrane transport would be greatly strengthened, and g_{liq} would markedly increase.

In addition, the recoveries of g_m and g_{sc} might also be greatly affected by leaf hydraulic conductivity (K_{leaf}) (Resco et al., 2009), as g_m and g_{sc} both showed correlations with leaf K_{leaf} in relevant studies (Flexas et al., 2013; Xiong et al., 2015b). Furthermore, Wang et al. (2018) revealed that leaf hydraulic vulnerability triggered declines in g_m and g_{sc} during periods of drought. In this study, increases in leaf Ψ_{pd} and AQP activity after rewatering indicated an increase in leaf K_{leaf}, which not only greatly improved leaf water supply and transport capacities but also strengthened CO_2 diffusion, as leaf water supply capacity was strongly related to leaf K_{leaf} and there was much overlap between the processes of water transport from vessel to stomata and CO_2 transport from the atmosphere to chloroplasts (Flexas et al., 2013; Xiong et al., 2017, 2015b). The hormonal and hydraulic signals involved in stomatal closure might be activated, followed by an increase in the and stomatal opening status (Sperry et al., 2002; Buckley, 2005; Dodd, 2005; Brodribb and Cochard, 2009; Rodriguez-Dominguez et al., 2016; McAdam and Brodribb, 2016). Furthermore, since changes in hormone levels (such as abscisic acid, ABA) and leaf structural properties may potentially affect g_m (Tombesi et al., 2015; Coupel-Ledru et al., 2017), soil rewatering might improve hormones and in turn promote g_m recovery. Thus, the g_m and g_{sc} recoveries might also be indirectly promoted by an increase in leaf K_{leaf}.

A detailed understanding to the coordination of AQP and CA activities and leaf anatomical characteristics could clarify the mechanisms of g_m and g_{sc} recoveries. Further studies are needed to understand the developmental basis for this coordination under dynamic environmental conditions.

5. Conclusion

Soil rewatering led to partial recoveries of g_m and g_{sc}, but the recoveries decreased with initial water stress in both species. In addition, the recoveries also varied between Manchurian ash and Mongolian oak saplings. The g_m recovery in Mongolian oak was much larger than that in Manchurian ash, while the g_{sc} obtained a larger recovery in Manchurian ash. The recovery of neither g_m nor g_{sc} was significant between July and August ($P < 0.05$). Photosynthesis recovery in Manchurian ash saplings was mostly affected by g_{sc} recovery, while that in Mongolian oak saplings was mostly affected by g_m recovery.

The g_m and g_{sc} recoveries were well explained by changes in leaf anatomy and AQP and CA activities. Both S_{mes} and g_{ias} had negative effects on g_m recovery, but these effects were largely compensated for by great increases in T_{leaf}, T_{mes} and g_{liq}. Consequently, the g_m recovery should mainly result from the great increase in g_{liq} after rewatering. In addition, the g_{sc} recovery was greatly triggered by an increase in SS (PL and PW at the center of the stoma). Furthermore, the activities of both AQP and CA increased after rewatering, which improved CO_2 trans-membrane transport and greatly promoted g_m and g_{sc} recoveries.

Authors' contributions

The experiment was supervised by Dexin Guan. Kai Zhu, Fenghui Yuan, Anzhi Wang, Dexin Guan, Changjie Jin and Jiabing Wu designed the experiment. Kai Zhu, Hongxia Zhang and Hong Yang helped in performing the experiment. Kai Zhu analyzed the data and wrote the manuscript. Kai Zhu, Fenghui Yuan, Dexin Guan, Yushu Zhang and Jiabing Wu revised and corrected the draft manuscript.

Acknowledgements

This study was supported by the National Natural Science Foundation of China (Grant No. 41675112, 31670707, 31770755, 31400541).

Appendix A. Supplementary data

Supplementary data to this article can be found online at https://doi.org/10.1016/j.plaphy.2019.09.025.

References

Allen, Simon, Plattner, K., 2013. Climate change 2013: the physical science basis. An overview of the working group 1 contribution to the fifth assessment report of the intergovernmental panel on climate change (IPCC). Comput. Geom. 18, 95–123.

Blackman, C.J., Brodribb, T.J., Jordan, G.J., 2009. Leaf hydraulics and drought stress: response, recovery and survivorship in four woody temperate plant species. Plant Cell Environ. 32, 1584–1595.

Brien, M.J., Leuzinger, S., Philipson, C.D., Tay, J., Hector, A., 2014. Drought survival of tropical tree seedlings enhanced by non-structural carbohydrate levels. Nat. Clim. Chang. 4, 710–714.

Brodribb, T.J., Holbrook, N.M., 2004. Stomatal protection against hydraulic failure: a comparison of coexisting ferns and angiosperms. New Phytol. 162, 663–670.

Brodribb, T.J., McAdam, S.A.M., 2011. Passive origins of stomatal control in vascular plants. Science 331, 582–585.

Brodribb, T.J., Cochard, H., 2009. Hydraulic failure defines the recovery and point of death in water-stressed conifers. Plant Physiol. 149, 575–584.

Buckley, T.N., 2005. The control of stomata by water balance. New Phytol. 168, 275–292.

Cano, F.J., López, R., Warren, C.R., 2014. Implications of the mesophyll conductance to CO_2 for photosynthesis and water-use efficiency during long-term water stress and recovery in two contrasting *Eucalyptus* species. Plant Cell Environ. 37, 2470–2490.

Chaves, M.M., Flexas, J., Pinheiro, C., 2009. Photosynthesis under drought and salt stress: regulation mechanisms from whole plant to cell. Ann. Bot. 103, 551–560.

Chartzoulakis, K., Patakas, A., Kofidis, G., 2002. Water stress affects leaf anatomy, gas exchange, water relations and growth of two avocado cultivars. Sci. Hortic. 95, 39–50.

Cai, Y.F., Wang, J.H., Li, S.F., 2015. Photosynthetic response of an alpine plant, *rhododendrondelavayi* Franch, to water stress and recovery: the role of mesophyll conductance. Front. Plant Sci. 6, 2707–2719.

Cavender-Bares, J., Bazzaz, F.A., 2000. Changes in drought response strategies with ontogeny in *Quercus rubra*: implications for scaling from seedlings to mature trees. Oecologia 124, 8–18.

Coupel-Ledru, A., Tyerman, S.D., Masclef, D., Lebon, E., Christophe, A., Edwards, E.J., Simonneau, T., 2017. Abscisic acid down-regulates hydraulic conductance of grapevine leaves in isohydric genotypes only. Plant Physiol. 175, 1121–1134.

Dore, M.H.I., 2005. Climate change and changes in global precipitation patterns: what do we know? Environ. Int. 31, 1167–1181.

Dodd, I.C., 2005. Root-to-shoot signalling: assessing the roles of 'up' in the up and down world of long-distance signalling *in planta*. Plant Soil 274, 251–270.

Epron, D., Godard, D., Cornic, G., Genty, B., 1995. Limitation of net CO_2 assimilation rate by internal resistances to CO_2 transfer in the leaves of two tree species (*Fagus sylvatica* L. and *Castanea sativa* Mill.). Plant Cell Environ. 18, 43–51.

Evans, J.R., von Caemmerer, S., Setchell, B.A., Hudson, G.S., 1994. The relationship between CO_2 transfer conductance and leaf anatomy in tobacco transformed with a reduced content of Rubisco. Aust. J. Plant Physiol. 21, 475–495.

Evans, J.R., Kaldenhoff, R., Genty, B., Terashima, I., 2009. Resistances along the CO_2 diffusion pathway inside leaves. J. Exp. Bot. 60, 2235–2248.

Flexas, J., Ribas-Carbó, M., Diaz-Espejo, A., Galmés, J., Hipólito, M., 2008. Mesophyll conductance to CO_2: current knowledge and future prospects. Plant Cell Environ. 31, 602–621.

Flexas, J., Barón, M., Bota, J., Ducruet, J.M., Gallé, A., Galmés, J., Jiménez, M., Pou, A., Ribas-Carbó, M., Sajnani, C., 2009. Photosynthesis limitations during water stress acclimation and recovery in the drought-adapted *Vitis* hybrid Richter-110 (*V. berlandieri* × *V. rupestris*). J. Exp. Bot. 60, 2361–2377.

Flexas, J., Bota, J., Escalona, J.M., Sampol, B., Medrano, H., 2002. Effects of drought on photosynthesis in grapevines under field conditions: an evaluation of stomatal and mesophyll limitations. Funct. Plant Biol. 29, 461–471.

Flexas, J., Bota, J., Galmés, J., Medrano, H., Ribas-Carbó, M., 2006. Keeping a positive carbon balance under adverse conditions: responses of photosynthesis and respiration to water stress. Physiol. Plant. 127, 343–352.

Flexas, J., Barbour, M.M., Brendel, O., 2012. Mesophyll diffusion conductance to CO_2: an unappreciated central player in photosynthesis. Plant Sci. 193–194, 70–84.

Flexas, J., Scoffoni, C., Gago, J., Sack, L., 2013. Leaf mesophyll conductance and leaf hydraulic conductance: an introduction to their measurement and coordination. J. Exp. Bot. 64, 3965–3981.

Field, C.B., Mooney, H.A., 1986. The photosynthesis-nitrogen relationship in wild plants. In: Givnish, T.J. (Ed.), On the Economy of Plant Form and Function. Cambridge University Press, Cambridge, UK, pp. 25–55.

Fredericksen, T.S., Joyce, B.J., Skelly, J.M., Steiner, K.C., Kolb, T.E., Kouterick, K.B., Savage, J.E., Snyder, K.R., 1995. Physiology, morphology, and ozone uptake of leaves of black cherry seedlings, saplings, and canopy trees. Environ. Pollut. 89, 273–283.

Fredericksen, T.S., Skelly, J.M., Steiner, K.C., Kolb, T.E., Kouterick, K.B., 1996. Size-mediated foliar response to ozone in black cherry trees. Environ. Pollut. 91, 53–63.

Fleischmann, F., Koehl, J., Portz, R., Beltrame, A.B., Oßwald, W., 2005. Physiological change of *Fagus sylvatica* seedlings infected with *Phytophthora citricola* and the contribution of its elicitin "Citricolin" to pathogenesis. Plant Biol. 7, 650–658.

Fleischmann, F., Winkler, J.B., Oßwald, W., 2009. Effects of ozone and *Phytophthora citricola* on non-structural carbohydrates of European beech (*Fagus sylvatica*) saplings. Plant Soil 323, 75–84.

Guyot, G., Scoffoni, C., Sack, L., 2012. Combined impacts of irradiance and dehydration on leaf hydraulic conductance: insights into vulnerability and stomatal control. Plant Cell Environ. 35, 857–871.

Galmés, J., Medrano, H., Flexas, J., 2007. Photosynthetic limitations in response to water stress and recovery in Mediterranean plants with different growth forms. New Phytol. 175, 81–93.

Galle, A., Florez-Sarasa, I., Tomas, M., 2009. The role of mesophyll conductance during water stress and recovery in tobacco (*Nicotiana sylvestris*): acclimation or limitation? J. Exp. Bot. 60, 2379–2390.

Galle, A., Haldimann, P., Feller, U., 2007. Photosynthetic performance and water relations in young pubescent oak (*Quercuspubescens*) trees during drought stress and recovery. New Phytol. 174, 799–810.

Genty, B., Briantais, J.M., Baker, N.R., 1989. The relationship between the quantum yield of photosynthetic electron-transport and quenching of chlorophyll fluorescence. Biochim. Biophys. Acta 990, 87–92.

Grassi, G., Magnani, F., 2005. Stomatal, mesophyll conductance and biochemical limitations to photosynthesis as affected by drought and leaf ontogeny in ash and oak trees. Plant Cell Environ. 28, 834–849.

Gillon, J.S., Yakir, D., 2000. Internal conductance to CO_2 diffusion and $C^{18}OO$ discrimination in C_3 leaves. Plant Physiol. 123, 201–214.

Guo, S.W., Kaldenhoff, R., Uehlein, N., Sattelmacher, B., Brueck, H., 2007. Relationship between water and nitrogen uptake in nitrate- and ammonium-supplied *Phaseolus vulgaris* L. plants. J. Plant Nutr. Soil Sci. 170, 73–80.

Haldimann, P., Galle, A., Feller, U., 2008. Impact of an exceptionally hot dry summer on photosynthetic traits in oak (*Quercus pubescens*) leaves. Tree Physiol. 28, 785–795.

Harley, P.C., Loreto, F., Marco, G.D., Sharkey, T.D., 1992. Theoretical considerations when estimating the mesophyll conductance to CO_2 flux by analysis of the response of photosynthesis to CO_2. Plant Physiol. 98, 1429–1436.

Han, J.M., Zhang, Y., Zhang, Y.J., Yi, X.P., Zhang, W.F., Zhang, Y.L., 2018. Drought-introduced variability of mesophyll conductance in Gossypium and its relationship with leaf anatomy. Physiol. Plant. 166, 873–887.

Hanba, Y.T., Shibasaka, M., Hayashi, Y., Hayakawa, T., Kasamo, K., Terashima, I., Katsuhara, M., 2004. Overexpression of the barley aquaporin HvPIP 2;1 increases internal CO_2 conductance and CO_2 assimilation in the leaves of transgenic rice plants. Plant Cell Physiol. 45, 521–529.

Heckwolf, M., Pater, D., Hanson, D.T., Kaldenhoff, R., 2011. The *Arabidopsis thaliana* aquaporin *At*PIP1;2 is a physiologically relevant CO_2 transport facilitator. Plant J. 67, 795–804.

Joos, F., Spahni, R.E., 2008. Rates of change in natural and anthropogenic radiative forcing over the past 20,000 years. Proc. Natl. Acad. Sci. 105, 1425–1430.

Kaldenhoff, R., Ribas-Carbó, M., Sans, J.F., Lovisolo, C., Heckwolf, M., Uehlein, N., 2008. Aquaporins and plant water balance. Plant Cell Environ. 31, 658–666.

Kawaletz, H., Mölder, I., Annighöfer, P., Terwei, A., Zerbe, S., Ammer, C., 2014. Pot experiments with woody species-A review. Forestry 87, 482–491.

Kunz, J., Räder, A., Bauhus, J., 2016. Effects of drought and rewatering on growth and gas exchange of minor European broadleaved tree species. Forests 7, 239.

Kolb, T.E., Fredericksen, T.S., Steiner, K.C., Skelly, J.M., 1997. Issues in scaling tree size and age responses to ozone: a review. Environ. Pollut. 98, 195–208.

Lawlor, D.W., Cornic, G., 2002. Photosynthetic carbon assimilation and associated metabolism in relation to water deficits in higher plants. Plant Cell Environ. 25, 275–294.

Luterbacher, J., Dietrich, D., Xoplaki, E., Grosjean, M., Wanner, H., 2004. European seasonal and annual temperature variability, trends, and extremes since 1500. Science 303, 1499–1503.
Loriaux, S.D., Avenson, T.J., Welles, D.K., 2013. Closing in on maximum yield of chlorophyll fluorescence using a single multiphase flash of sub-saturating intensity. Plant Cell Environ. 36, 1755–1770.
Laisk, A.K., 1977. Kinetics of Photosynthesis and Photorespiration of C_3 Plants. Mccarthy.
Monclus, R., Dreyer, E., Villar, M., Delmotte, F.M., Delay, D., Petit, J.M., Barbaroux, C., Thiec, D., Brechet, C., Brignolas, F., 2006. Impact of drought on productivity and water use efficiency in 29 genotypes of *Populusdeltoides* × *Populusnigra*. New Phytol. 169, 765–777.
McAdam, S.A., Brodribb, T.J., 2013. Ancestral stomatal control results in a canalization of fern and lycophyte adaptation to drought. New Phytol. 198, 429–441.
McAdam, S.A., Brodribb, T.J., 2016. Linking turgor with ABA biosynthesis: implications for stomatal responses to vapor pressure deficit across land plants. Plant Physiol. 171, 2008–2016.
Mahdieh, M., Mostajeran, A., Horie, T., Katsuhara, M., 2008. Drought stress alters water relations and expression of PIP-type aquaporin genes in Nicotiana tabacum plants. Plant Cell Physiol. 49, 801–813.
Miyazawa, S.I., Yoshimura, S., Shinzaki, Y., Maeshima, M., Miyake, C., 2008a. Relationship between mesophyll conductance to CO_2 diffusion and contents of aquaporin localized at plasma membrane in tobacco plants grown under drought conditions. In: Allen, J.F., Gantt, E., Golbeck, J.H., Osmond, B. (Eds.), Photosynthesis: Energy from the Sun. Springer, New York, pp. 805–808.
Miyazawa, S.I., Yoshimura, S., Shinzaki, Y., Maeshima, M., Miyake, C., 2008b. Deactivation of aquaporins decreases internal conductance to CO_2 diffusion in tobacco leaves grown under long-term drought. Funct. Plant Biol. 35, 553–564.
Maeda, Y., Smith, B.L., Agre, P., Knepper, M.A., 1995. Quantification of aquaporin-CHIP water channel protein in microdissected renal tubules by fluorescence-based ELISA. J. Clin. Investig. 95, 422–428.
Mori, I.C., Rhee, J., Shibasaka, M., Sasano, S., Kaneko, T., Horie, T., Katsuhara, M., 2014. CO_2 transport by PIP2 aquaporins of barley. Plant Cell Physiol. 55, 251–257.
Niinemets, Ü., Reichstein, M., 2003. Controls on the emission of plant volatiles through stomata: a sensitivity analysis. J. Geophys. Res. 108, 4211.
Niinemets, Ü., 2010. Responses of forest trees to single and multiple environmental stresses from seedlings to mature plants: past stress history, stress interactions, tolerance and acclimation. For. Ecol. Manag. 260, 1623–1639.
Nunn, A.J., Kozovits, A.R., Reiter, I.M., Heerdt, C., Leuchner, M., Lütz, C., Liu, X., Löw, M., Winkler, J.B., Grams, T.E.E., Häberle, K.H., Werner, H., Fabian, P., Rennenberg, H., Matyssek, R., 2005. Comparison of ozone uptake and sensitivity between a phytotron study with young beech and a field experiment with adult beech (*Fagus sylvatica*). Environ. Pollut. 137, 494–506.
Ocheltree, T.W., Nippert, J.B., Prasad, P.V.V., 2012. Changes in stomatal conductance along grass blades reflect changes in leaf structure. Plant Cell Environ. 35, 1040–1049.
Pons, T.L., Flexas, J., von Caemmerer, S., Evans, J.R., Genty, B., Ribas-Carbo, M., Brugnoli, E., 2009. Estimating mesophyll conductance to CO_2: methodology, potential errors, and recommendations. J. Exp. Bot. 60, 2217–2234.
Perez-Martin, A., Torres-Ruiz, J.M., Fernández, J.E., Diaz-Espejo, A., Flexas, J., Michelazzo, C., 2011. Physiological and genetic response of olive leaves to water stress and recovery: implications of mesophyll conductance and genetic expression of aquaporins and carbonic anhydrase. Acta Hortic. (Wagening.) 922, 99–105.
Perez-Martin, A., Michelazzo, C., Torres-Ruiz, J.M., Flexas, J., Fernández, J.E., 2014. Regulation of photosynthesis and stomatal and mesophyll conductance under water stress and recovery in olive trees: correlation with gene expression of carbonic anhydrase and aquaporins. J. Exp. Bot. 65, 3143–3156.
Quick, W.P., Chaves, M.M., Wendler, R., David, M., Rodrigues, M.L., Passaharinho, J.A., Pereira, J.S., Adcock, M.D., Leegood, R.C., Stitt, M., 1992. The effect of water stress on photosynthetic carbon metabolism in four species grown under field conditions. Plant Cell Environ. 15, 25–35.
Rho, H., Yu, D.J., Su, J.K., Lee, H.J., 2012. Limitation factors for photosynthesis in 'Bluecrop' highbush blueberry (*Vaccinium corymbosum*) leaves in response to moderate water stress. J. Plant Biol. 55, 450–457.
Resco, V., Ewers, B.E., Sun, W., Huxman, T.E., Weltzin, J.F., Williams, D.G., 2009. Drought-induced hydraulic limitations constrain leaf gas exchange recovery after precipitation pulses in the C_3 woody legume, Prosopis velutina. New Phytol. 181, 672–682.
Rodriguez-Dominguez, C.M., Buckley, T.N., Egea, G., de Cires, A., Hernandez-Santana, V., Martorell, S., Diaz-Espejo, A., 2016. Most stomatal closure in woody species under moderate drought can be explained by stomatal responses to leaf turgor. Plant Cell Environ. 39, 2014–2026.
Sun, J.W., Guan, D.X., Wu, J.B., Jin, Y.L., Yuan, F.H., Wang, A.Z., Jin, C.J., 2015. Day and night respiration of three tree species in a temperate forest of northeastern China. iFor. Biogeosci. For. 8, 25–32.
Sade, N., Gallé, A., Flexas, J., Lerner, S., Peleg, G., Yaaran, A., Moshelion, M., 2014. Differential tissue-specific expression of *NtAQP1* in *Arabidopsis thaliana* reveals a role for this protein in stomatal and mesophyll conductance of CO_2 under standard and salt-stress conditions. Planta 239, 357–366.
Syvertsen, J.P., Lloyd, J., McConchie, C., Kriedemann, P.E., Farquhar, G.D., 1995. On the relationship between leaf anatomy and CO_2 diffusion through the mesophyll of hypostomatous leaves. Plant Cell Environ. 18, 149–157.
Samuelson, L., Michael Kelly, J., 2001. Scaling ozone effects from seedlings to forest trees. New Phytol. 149, 21–41.
Sperry, J.S., Hacke, U.G., Oren, R., Comstock, J.P., 2002. Water deficits and hydraulic limits to leaf water supply. Plant Cell Environ. 25, 251–263.
Tholen, D., Boom, C., Noguchi, K., Ueda, S., Katase, T., Terashima, I., 2008. The chloroplast avoidance response decreases internal conductance to CO_2 diffusion in *Arabidopsis thaliana* leaves. Plant Cell Environ. 31, 1688–1700.
Tosens, T., Niinemets, U., Vislap, V., Eichelmann, H., Castro, D.P., 2012. Developmental changes in mesophyll diffusion conductance and photosynthetic capacity under different light and water availabilities in *Populustremula*: how structure constrains function. Plant Cell Environ. 35, 839–856.
Tosens, T., Nishida, K., Gago, J., Coopman, R.E., Cabrera, H.M., Carriqui, M., Laanisto, L., Morales, L., Nadal, M., Rojas, R., 2016. The photosynthetic capacity in 35 ferns and fern allies: mesophyll CO_2 diffusion as a key trait. New Phytol. 209, 1576–1590.
Tomás, M., Flexas, J., Copolovici, L., Galmés, J., Hallik, L., Medrano, H., 2013. Importance of leaf anatomy in determining mesophyll diffusion conductance to CO_2 across species: quantitative limitations and scaling up by models. J. Exp. Bot. 64, 2269–2281.
Thain, J.F., 1983. Curvature correction factors in the measurement of cell surface areas in plant tissues. J. Exp. Bot. 34, 87–94.
Tu, M.X., Wang, X.H., Feng, T.Y., Sun, X.M., Wang, Y.Q., Huang, L., Gao, M., Wang, Y.J., Wang, X.P., 2016. Expression of a grape (*Visits vinifera*) bZIP transcription factor, VIbZIP36, in *Arabidopsis thaliana* confers tolerance of drought stress during seed germination and seedling establishment. Plant Sci. 252, 311–323.
Tombesi, S., Nardini, A., Frioni, T., Soccolini, M., Zadra, C., Farinelli, D., Poni, S., Palliotti, A., 2015. Stomatal closure is induced by hydraulic signals and maintained by ABA in drought-stressed grapevine. Sci. Rep. 5, 12449.
Uehlein, N., Otto, B., Hanson, D.T., Fischer, M., McDowell, N., Kaldenhoff, R., 2008. Function of Nicotiana tabacum aquaporins as chloroplast gas pores challenges the concept of membrane CO_2 permeability. Plant Cell 20, 648–657.
Uehlein, N., Lovisolo, C., Siefritz, F., Kaldenhoff, R., 2003. The tobacco aquaporin NtAQP1 is a membrane CO_2 pore with physiological functions. Nature 425, 734–737.
von Caemmerer, S., Evans, J., Hudson, G., Andrews, T.J., 1994. The kinetics of ribulose-1,5-bisphosphate carboxylase/oxygenase in vivo inferred from measurements of photosynthesis in leaves of transgenic tobacco. Planta 195, 88–97.
von Caemmerer, S., Farquhar, G.D., 1981. Some relationships between the biochemistry of photosynthesis and the gas exchange of leaves. Planta 153, 376–387.
Valentini, R., Epron, D., De Angelis, P., Matteucci, G., Dreyer, E., 1995. In situ *estimation of net CO2 assimilation, photosynthetic electron flow and photorespiration in Turkey oak (Q. cerris* L.) leaves: diurnal cycles under different levels of water supply. Plant Cell Environ. 18, 631–640.
Warren, C.R., 2006. Estimating the internal conductance to CO_2 movement. Funct. Plant Biol. 33, 431–442.
Wang, X.X., Du, T.T., Huang, J.L., Peng, S.B., Xiong, D.L., 2018. Leaf hydraulic vulnerability triggers the decline in stomatal and mesophyll conductance during drought in rice. J. Exp. Bot. 16, 4033–4045.
Xiong, D.L., Xi, L., Liu, L.M., Douthe, C., Li, Y., Peng, S.B., Huang, J.L., 2015a. Rapid responses of mesophyll conductance to changes of CO_2 concentration, temperature and irradiance are affected by N supplements in rice. Plant Cell Environ. 38, 2541–2550.
Xiong, D.L., Flexas, J., Yu, T.T., Peng, S.B., Huang, J.L., 2017. Leaf anatomy mediates coordination of leaf hydraulic conductance and mesophyll conductance to CO_2 in *Oryza*. New Phytol. 213, 572–583.
Xiong, D.L., Yu, T.T., Zhang, T., Li, Y., Peng, S.B., Huang, J.L., 2015b. Leaf hydraulic conductance is coordinated with leaf morpho-anatomical traits and nitrogen status in the genus *Oryza*. J. Exp. Bot. 66, 741–748.